Climate Dynamics (2019) 52:6691–6704
https://doi.org/10.1007/s00382-018-4540-5

Improved performance of a PRECIS ensemble in simulating near-surface air temperature over China

Junhong Guo[1] · **Guohe Huang**[2,3] · **Xiuquan Wang**[4] · **Yongping Li**[5]

Received: 23 June 2018 / Accepted: 14 November 2018 / Published online: 23 November 2018
© Springer-Verlag GmbH Germany, part of Springer Nature 2018

Abstract

The near-surface air temperature over China is simulated from 1950 to 2099 using the PRECIS model from the Met Office Hadley Centre at a 25-km resolution. In order to reflect the different parametric and structural uncertainties in future temperature projections, the PRECIS model is driven by five lateral boundary conditions, which include a four-member HadCM3-based perturbed-physics ensemble (i.e., HadCM3Q0, Q1, Q7 and Q13) and an ECHAM5 model. For the present climate, PRECIS reasonably reproduces the spatial patterns of near-surface air temperatures over most regions in China, except for some underestimation in the west. The annual cycles of mean temperature are well captured but its magnitude is slightly underestimated throughout the year. Future temperature projections are further analyzed for three successive 30-year periods throughout the twenty-first century. Despite more uncertainties with time, the ensemble results demonstrate that the temperature over China is likely to continue to increase throughout the twenty-first century, with different spatial-time variation. There is an apparent increasing pattern along with the latitude for seasonal temperature. Through comparison with the driving GCMs, PRECIS ensemble shows smaller biases in most regions of China, except for in the west plateau. The cause is that RCMs could inherit some errors from the driving GCMs in addition to their own errors. These errors could be magnified unintentionally in downscaling over high elevations and have been propagated into future climate projections. However, there is no apparent relationship between projected changes and model biases (i.e., larger bias does not necessarily lead to bigger changes in temperature). These results could be directly used to analyze the impacts caused by climate warming on agriculture, energy and other related sectors in China.

Keywords Temperature changes · China · High resolution · Regional climate model ensemble

1 Introduction

Assessing the potential impacts of global warming and accurate prediction of future climate change have been an important interest to researchers and policy makers, in order to develop targeted public policies and measures for adaptation and mitigation (Adger et al. 2005). Global climate models (GCMs) are an important aspect of climate change research and are used to generate projections of how the climate may change in the future. However, GCMs which run at a global scale with a coarse resolution (usually over 100 km) do not adequately assess the impact or capture larger deviations that may occur at regional levels. Therefore, further downscaling through regional climate models (RCMs) should be used to transfer large-scale climate changes to local weather series at finer spatial and temporal resolutions (Buontempo et al. 2014; Guo et al. 2017; Wang et al. 2015).

Generally, a main downscaling method is to build a math-statistics mapping or relationship between the large-scale coarse atmospheric variables (i.e., predictors) and local weather variables (i.e., predictands). Statistical downscaling has been widely applied to the field of climate research by virtue of easier implementation, lower computing costs and achievable site-specific information (Guo et al. 2017; Wang et al. 2014a, 2015). However, owing to overwhelming dependence on present day climate factors, the relationship between predictors and predictands in statistical

Electronic supplementary material The online version of this article (https://doi.org/10.1007/s00382-018-4540-5) contains supplementary material, which is available to authorized users.

✉ Guohe Huang
huang@iseis.org

✉ Xiuquan Wang
xiuquan.wang@gmail.com

Extended author information available on the last page of the article

downscaling is empirical and theoretical assertion, which may not hold in the future climate. Comparatively, dynamical downscaling is usually driven by given time-varying boundary conditions from GCMs to generate finer-resolution grids. In other words, RCMs have the same physical processes and mechanism as described in GCMs and can agree better with the local situation (Redmond et al. 2015). RCMs using dynamical downscaling techniques have attracted attention in climate model research in recent years (Boé et al. 2007; Liu et al. 2013; Wang et al. 2014a).

Increasing attention has been paid to climate simulations and projections in China in recent years. Some studies compared and analyzed the outputs from large GCM ensembles directly (Ouyang et al. 2015), while others focused on certain specific climatic regions, for example in the northwest (Shi et al. 2003, 2007), the east (Chen et al. 2005) and the south (Di et al. 2010; Huang et al. 2013). In respect of using regional climate models in simulation over China, Gao et al. (2012a) used RegCM3, nested within the global model CCSR/NIES/FRCGC MIROC3.2_hires, to analyze the climate change in the twenty-first century over China. Similarly, Liu et al. (2013) used the same RCM but nested with different GCM (CCSM) to investigate the changes in precipitation and surface air temperature in future. Yu et al. (2014) employed WRF climate model to evaluate the performance of a long high-resolution (30 km) continuous simulation in climatology and extremes over China based on multiple observations. Wang et al. (2014b) explored the time-lagged impact of the spring sensible heat source over the Tibetan Plateau on the summer rainfall anomaly in eastern China using WRF. However, these studies also more or less have some inadequacies, such as short simulation periods, coarse spatial resolution, more uncertainties and so on, especially in the latter two, which are vital to provide direct inputs for further climate change impact assessment and adaptation studies in regional scale. Specifically, coarse spatial resolution cannot represent more detailed information in a spatial grid, which could result in more biases in simulation and projection, particularly in complex terrains. On the other hand, single climate model is not incapable to project the climate change, and the corresponding results are often not very reliable and should be interpreted with caution owing to various uncertainties (Yu et al. 2014).

Therefore, the objective of this study is to investigate the long-term climate change over the entire country of China with consideration of regional variations through high-resolution climate simulations. Specifically, the near-surface air temperature over China was simulated throughout the twenty-first century using the PRECIS model with a spatial resolution of 25 km. The PRECIS model was driven by a five-member ensemble of lateral boundary conditions to account for the uncertainties of future climate projections. This will help capture the most likely spread of temperature changes until the end of this century for the entire country at local scales.

2 Data and methods

2.1 Validation methods

To evaluate the model's performance, an observational gridded and unrestricted temperature dataset was used. The dataset is derived from the APHRODITE project, namely, Asian Precipitation-Highly-Resolved Observational Data Integration Towards Evaluation of Water Resources (hereinafter referred to as APHRO), which develops state-of-the-art near surface meteorology (mainly precipitation and temperature) with high-resolution grids for Asia (Hamada et al. 2011). The latest released daily mean temperature product is AphroTemp_V1204R1 version for the period 1961–2007 at 0.25° grid (see: http://www.chikyu.ac.jp/precip/english/scope.html). We extracted a consecutive data record for our model domain as the comparison in this study.

In order to quantify the performance of PRECIS during the baseline period, we calculated the correlation coefficient, the centered pattern root-mean-square difference and the ratio of standard deviations between simulations and observation. Thus, a Taylor diagram is applied to present these characteristics comprehensively and visually (Taylor 2001; Jiang et al. 2015).

2.2 Regional climate modeling

The PRECIS, developed by the Met Office Hadley Center, is the one of the widely-used RCMs for global regional climate simulations (i.e., Wang et al. 2014a, 2015; Buontempo et al. 2014; Guo et al. 2018). PRECIS is an atmosphere and land surface model of limited area and has two high resolutions, which are 0.44°×0.44° (~ 50 km) and 0.22° × 0.22° (~ 25 km) at the equator of the rotated regular latitude-longitude grid. It contains 19 levels in a vertical hybrid-coordinate system and can be applied to generate high-resolution climate change information for as many regions of the world as possible. Its driving LBCs have horizontal resolution of 3.75° longitude (~ 400 km) and 2.5° latitude (~ 300 km). The land surface scheme in this study is MOSES 2.2 (Met Office Surface Exchange Scheme).

PRECIS provides a based perturbed physics technology to quantify uncertainties in model projections (known as QUMP) under the IPCC SRES A1B emissions scenario. The QUMP ensemble consists of 17 members (HadCM3Q0-Q16) and is used to generate a set of high-resolution regional climate projections (Wang et al. 2015; Collins et al. 2006), and each one has a set of perturbations to its unique dynamical and physical formulation (McSweeney et al. 2012).

However, if we entirely downscale the 17 members with PRECIS, it would be very expensive, requiring large inputs of computing resources, data storage and data analyses. In order to meet the requirements and explore a wide range of uncertainties, according to the Hadley Centre's recommendation, we select a subset of four members (i.e., HadCM3Q0, Q1, Q7 and Q13) from the ensemble of QUMP as the model's lateral boundary data (McSweeney and Jones 2010). The PRECIS model would be run from 1950 to 2099 at its highest spatial resolution of 25 km. In addition, another driving model with PRECIS is the Max Plank Institute's fifth generation coupled ocean–atmosphere general circulation model (ECHAM5), which is run for comparison and analysis. In general, the HadCM3 QUMPs are used to reflect the uncertainties associated with different parametric settings, while we also choose the ECHAM5 as the other GCM boundary to analyze the model structural uncertainties through comparison with the HadCM3 downscaled by the PRECIS. The simulation results for the period of 1961–1990 (referred to as the baseline period) are first compared to the APHRO dataset to depict the model biases and simulation performance. The results for the period of 2011–2099 from the PRECIS ensemble simulations are extracted and analyzed to help understand the likely outcomes of China's future climate.

In addition, followed the approach employed in the fifth generation of climate change information for the United Kingdom (UKCP09) (Murphy et al. 2009), we applied the interval analysis and cumulative distribution function (CDF) to explain future probability projections, instead of completely displaying the absolute result from each simulation. The probability of future temperature changes is defined as being less than or greater than a given amount. A cumulative probability of 10% is used to indicate the minimum acceptable level or lower bound of credibility interval, namely the actual value that is very likely to be greater than or very unlikely to be less than the given amount. In contrast, the cumulative probability of 90% is used to indicate the maximum acceptable level or upper bound of credibility, that is, the actual value is very likely to be less than or very unlikely to be greater than the current given value. In the same way, we regard the value with a cumulative probability of 50% as the most likely estimate of future projections.

2.3 Model domain

In this study, we configured a domain extending from about 66.24°E–139.48°E and 10.07°N–54.34°N with over 38,000 25-km grid points in total (Fig. 1). This reflects some external influences which play important roles in China's regional climatology, such as East Asian winter, summer and tropical oceanic monsoons. In addition, we selected four appropriate typical samples of climatic regimes (Table 1) across China to validate and project temperature data using the PRECIS model.

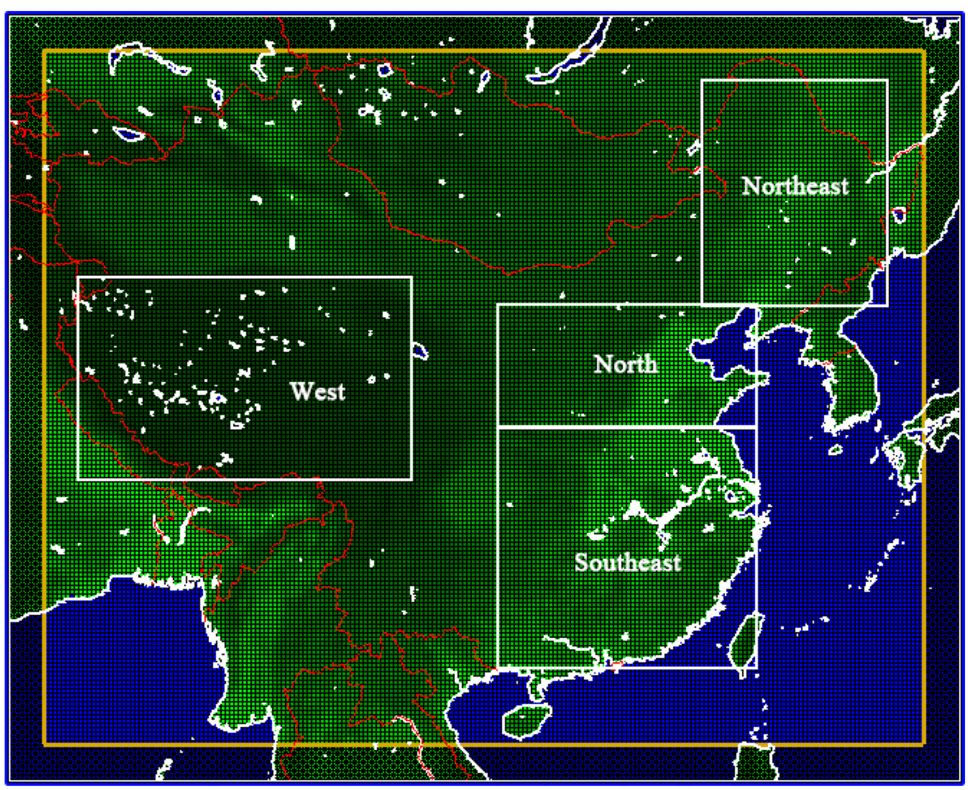

Fig. 1 PRECIS model domain. The buffer zone of 8 grids is between yellow and blue rectangle boxes. The blue grids represent sea area, while green ones are land area and the deeper the color, the higher altitude. There are 4 regions selected for validating across different climatic regions of China, which are Northeastern China (NE), Northern China (N), Southeastern China (SE) and Western China (W), respectively

Table 1 Coordinates of China regions

No.	Region	Longitude	Latitude
1	China	66.24°E–139.48°E	10.07°N–54.34°N
2	Northeast China	117.54°E–130.17°E	40°65′N–52°29′N
3	North China	104.4°E–121.34°E	34.92°N–40.06°N
4	Southeast China	105.68°E–21.14°E	22.82°N–33.98°N
5	West China	78.48°E–101.16°E	30.58°N–34.84°N

3 Results

3.1 Model validation

3.1.1 Spatial patterns of present-day climate

Overall, the PRECIS model reasonably reproduces the regional scale climatological temperature patterns across most regions of China aside from local differences, especially in western China. Figure 2 shows the geographic distribution of annual mean temperature in observation and simulations (including the driving GCMs and RCM ensemble mean) and their biases (simulations minus observation) during the baseline period. The major hot centers (the southeast and northwest) and cold centers (the northeast and the Tibet Plateau) are well simulated by PRECIS. The performance of PRECIS in the east is better than that in the west of China. The magnitude of the bias generally varies within the range of [− 2, 2] °C in most areas except in the Himalayan margin and southeastern parts of Tibet in China. Compared with the RCM ensemble, the results from their corresponding GCM simulations demonstrate differences in some regions. For example, negative anomalies are found in the northwest of Xinjiang and the northeast of China while the surrounding regions in the southern Xinjiang show considerable warm biases. The seasonal mean temperature in spatial distribution is similar with the annual mean temperature, and the main temperature centers and zones of China are captured well especially in spring (Figure S2 in supplemental materials) and autumn (Figure S4). However, the capability of GCM in reproducing the mean temperature is noticeably worse than RCM in winter (Figure S1), with sharply underestimation in most regions of China (i.e., exceeding 6 °C cold bias in northeast and west). But it should be noticed that the downscaled results show some warm biases are found in the northern Xinjiang in winter, while these biases move to the southern Xinjiang in summer (Figure S2). The significant cold biases are also found over the

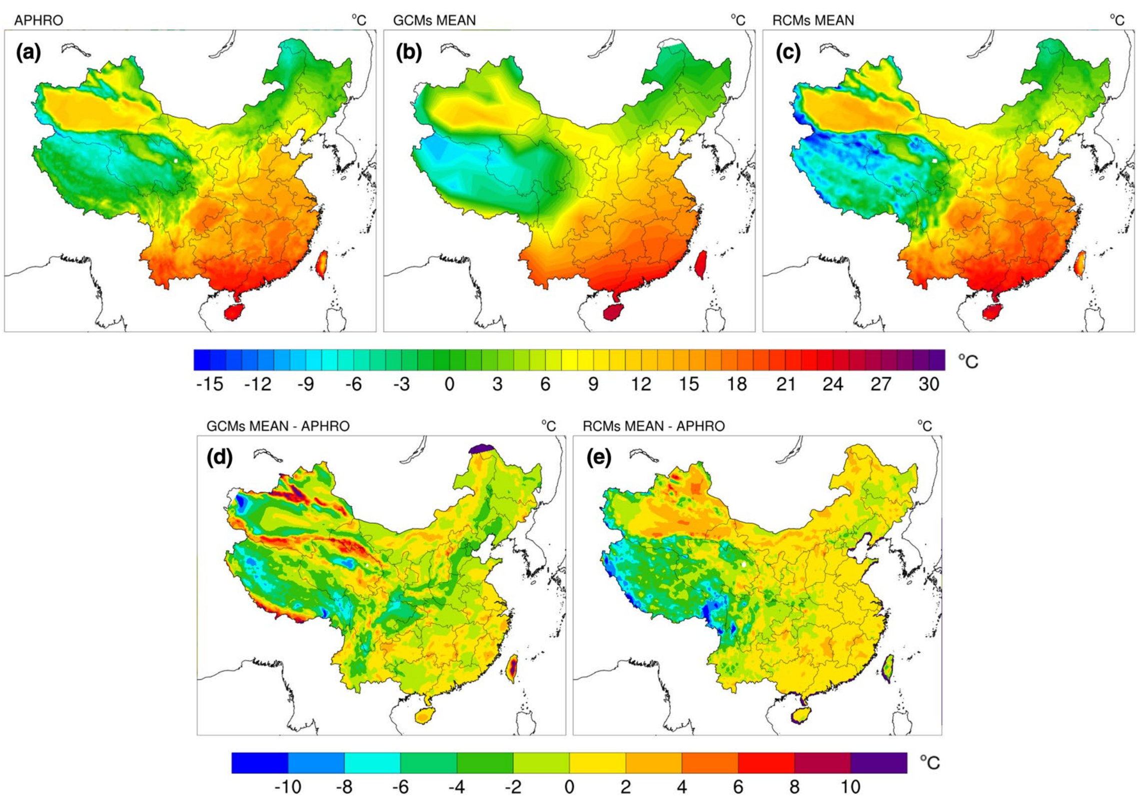

Fig. 2 Spatial distribution of annual mean temperature during the baseline period (1961–1990): **a** observation, **b** GCMs, **c** RCMs, **d** bias between GCMs and observation, and **e** bias between RCMs and observation

west or the Tibetan Plateau (especially in cold seasons), which are broadly consistent to those reported on previous studies over China (Gao et al. 2011b, 2015). There are common problems, such as complex land surface information, insufficient observations, inaccurate representation of snow processes and elevation dependent, which could result in poor performance and challenges in reproducing climate features over high topographic regions (Ouyang et al. 2015; Yu et al. 2014). Nevertheless, in comparison with single member of RCM runs or large-scale climate model, our results have some superiority in reginal details demonstration and uncertainty reduction.

To quantitatively evaluate the model's ability on simulating the pattern of the present-day mean temperature over China, we use Taylor diagram to characterize three assessment indicators mentioned above for annual and seasonal mean temperature during the baseline period over China and the sub-regions (Fig. 3). For the annual or seasonal mean temperature, the majority of RCM simulations have high pattern correlation coefficients and low centered pattern root-mean-square differences with observation in most regions except the west. For instance, the correlation coefficients are in the range of 0.85 and 0.99 and the centered pattern root-mean-square differences remain between 0.25 and 0.75, indicating the RCM ensemble has good simulated skills in simulating the pattern distribution of mean temperature. The simulation in the west is worse performance relative to other regions; however, the RMSE of GCMs is smaller than RCMs, especially in summer, indicating that the RCM ensemble has no satisfactory improvements in the western plateau regions (Fig. 7c). In addition, all simulations have good performances in the ratio of standard deviations between 0.75 and 1.25, indicating the simulated pattern variations are similar with observation. Nevertheless, the degree of phase agreement between RCMs and observation is higher than GCMs owing to the enhanced representation of the land surface boundary.

3.1.2 Annual cycle

Figure 4 shows the annual temperature cycles relative to observation as simulated by the RCM ensemble and their GCMs. The shape of mean temperature annual cycles is generally well reproduced by PRECIS ensemble simulations in all regions, although there are some differences in predefined regions.

For four sub-regions, the simulations from PRECIS overvalue the mean temperature in most months except for the west. Specifically, the warm bias in the northern China is larger than the south (Fig. 4f). There is a warm bias (exceeding 2 °C) in the cold months (January, February and March) and hot months (July and August) in the northeast (Fig. 4d). Relatively small bias between observation and the RCMs is in the southeastern China (Fig. 4h). The simulations of GCMs show similar biases over the three regions of eastern China (i.e., NE, N and SE), and colder biases are found in simulations by GCMs than RCMs, particularly in cold seasons. On the other hand, compared to the rest regions of China with weak positive biases, the mean temperature in the area of western China is completely underestimated with excessively negative biases in all months throughout the year, especially in winter (below − 5 °C). It explains why the mean temperature in the whole of China is underestimated: the warm biases that are relatively weak yet covering large part of China are overwhelmed by the very strong cool biases over relatively small area of western China. But it is worth noting that GCMs show relatively small biases in west than RCMs. This inconsistent performance in the eastern and western China from GCMs and RCMs can also be identified from aforementioned spatial distribution maps and Taylor diagram. As mentioned above, the possible reason of the poor performance simulated by RCMs in the western plateau is that they could inherit some errors from the driving GCMs in addition to their own errors, and these errors could be further magnified unintentionally in downscaling over high elevations (Liang et al. 2008).

3.2 Projections of future climate

Here we divided the simulated results into three continuous 30-year periods throughout the twenty-first century: 2011–2040 (or early-21st C), 2041–2070 (or mid-21st C), and 2071–2099 (or late-21st C). The projected spatial changes for three future periods with respect to baseline climate are discussed in the following sections.

3.2.1 Changes in spatial distribution

Figure 5 shows that in the early twenty-first century the projected results suggest that the most likely mean temperature range over the whole of China would be [1.3, 1.9] °C. Overall, the ensemble simulations project the largest warming regions in the north while the lower warming in the most southern China. The seasonal temperature shows gradually increasing pattern along with the latitude, especially in winter. For example, there is virtually no significant temperature change in southern Guangdong, Guangxi and Hainan regions in winter at 10% level, while in the northeast and northwest the temperature would largely increase by about 1.5 °C at 10% level and 3.0 °C at 90% level compared with the baseline period. Meanwhile, there is the smallest amplitude of change in spring. In this period, the possible warming ranges for the four seasons are [1.2, 2.3] °C in winter, [1.1, 2.0] °C in summer, [1.0, 1.8] °C in spring, [1.3, 2.0] °C in autumn, respectively.

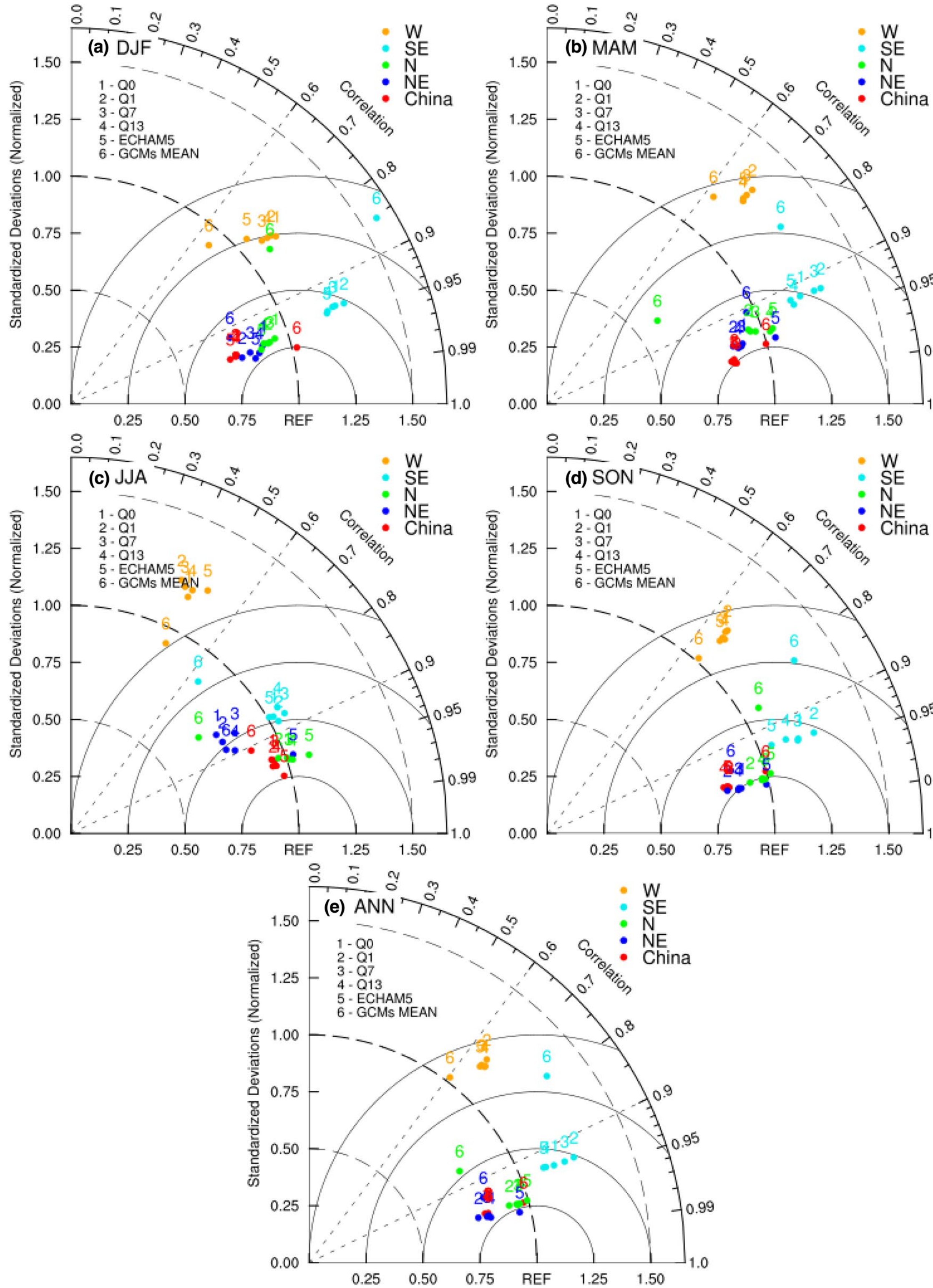

Fig. 3 Taylor diagrams of mean seasonal and annual temperature for simulations (1–5: RCMs; 6: GCMs) versus observation over the entire China and four sub-regions (NE, N, SE and W)

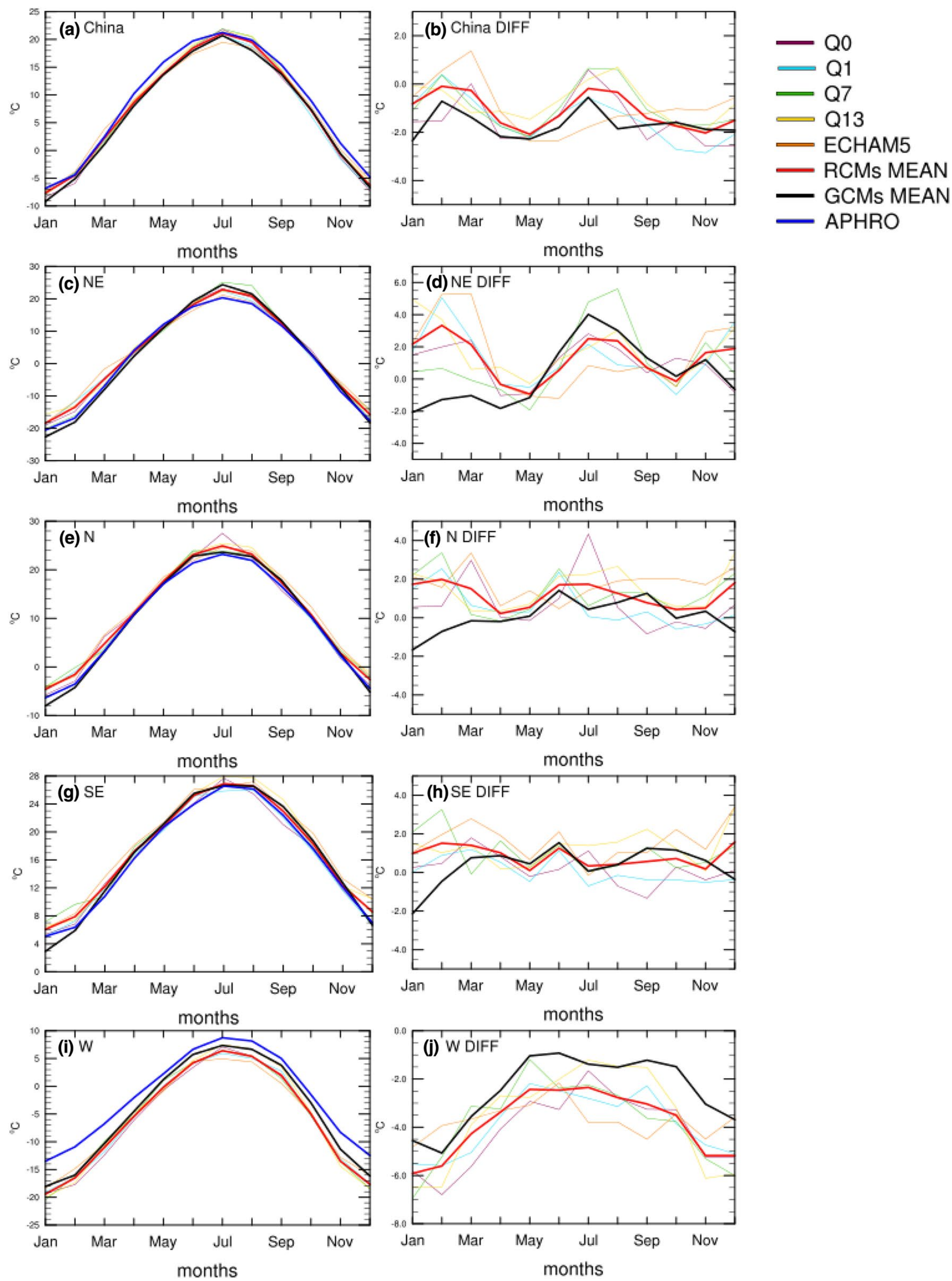

Fig. 4 Annual cycle of mean temperature (left) and biases (right) between simulations (black: GCMs mean; red: RCMs mean) and observation (blue) over China (**a, b**) and 4 sub-regions (**c**–**j**) during the baseline period (1961–1990)

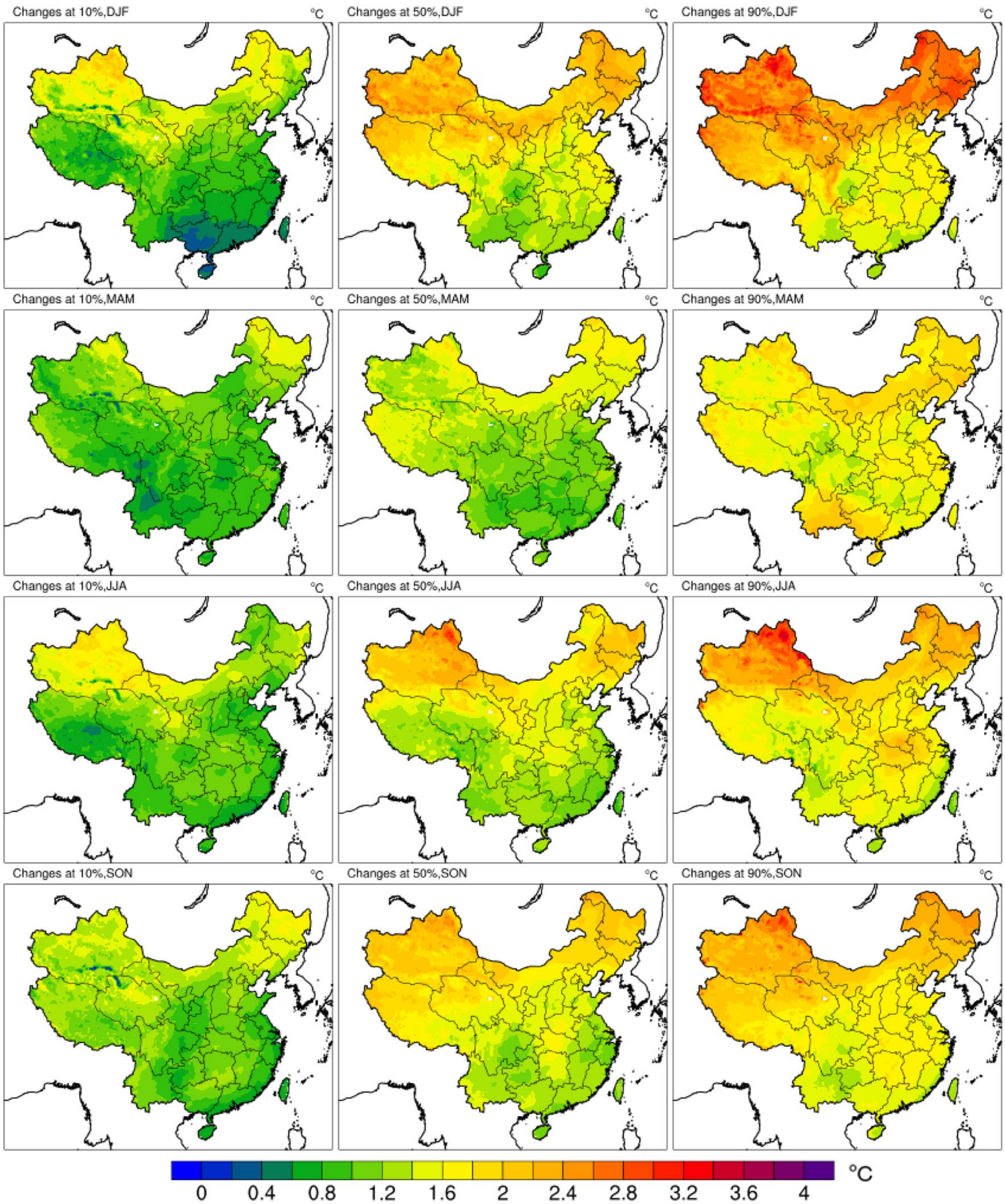

Fig. 5 Temperature changes in the early twenty-first century (2011–2040) at 10% probability level (left), 50% probability level (middle) and 90% probability level (right) compared to the baseline period (1961–1990): **a**–**c** winter, **d**–**f** spring, **g**–**i** summer, **j**–**l** autumn

By comparison with early twenty-first century, the overall temperature of the ensemble presents a continuous increase and the changes in the annual average temperature become larger in the mid-21st C, ranging from 2.5 °C at 10%, 3.2 at 50% to 3.7 °C at 90% CDF level (Figure S5). Except for spring, the mean temperature climbs more rapidly ([2.6, 3.9] °C) in the whole of China, and the warming is more pronounced in the northeast and northwest especially in winter and summer. By contrast, the lowest increase is in the southeast during spring ([2.0, 2.8] °C). Besides the latitude variation being consistent with the earlier period, the warming amplitude in the west is slightly high than the east in winter but low in summer.

The temperature change hovers in a wider range across China in the end of this century ([3.7, 5.2] °C), as shown in Figure S6. Consistent with the two former periods, the amplitude of temperature growth in the northern high latitude areas is increasing more than the south. The warming is more pronounced in winter while the smallest change is in spring for the entire China region. However, compared with the rapidly growth in the mid-twenty-first century, the rate of warming may slow down in this period, especially in summer and winter. The slowdown of warming in late-twenty-first century is consistent with the evolution of the anthropogenic forcing in A1B scenario, which describes a future of very rapid economic growth, greenhouse gas emissions that peaks in mid-century and declines thereafter.

Figure 6 shows the regional mean in mean temperature. There is a similar trend in spatial patterns, but the projected results present distinct features. According to the seasons, the increase is relatively smaller in spring than that in other seasons for all sub-regions, with the smallest increase (1.1 °C, 2.4 °C and 3.5 °C) in the southeast (Fig. 6d). The seasons of the largest increase in temperature are different. For example, a larger change is found in winter for the northeast (2.2 °C, 4.2 °C and 5.7 °C, Fig. 6b) and the west (1.8 °C, 3.4 °C and 4.8 °C, Fig. 6e). Similarly, other two sub-regions also show larger increase in winter in the early twenty-first century, with 1.8 °C for the north (Fig. 6c) and 1.4 °C for the southeast (Fig. 6d). However, in the middle and late twenty-first century, the increase in summer or autumn is slightly higher than other seasons. For example, the north shows 3.2 °C and 4.5 °C increase in summer while the southeast shows 2.8 °C and 4.1 °C increase in autumn. For the whole of China, the larger increase is most likely to appear in winter (1.8 °C, 3.4 °C and 4.8 °C), while the smaller is in spring (1.4 °C, 2.7 °C and 4.0 °C) (Fig. 6a).

The spatio-temporal changes in minimum and maximum temperature in the twenty-first century are presented in Figure S7. Overall, the close resemblance between the pattern change in extreme temperature and mean temperature is obvious, that is, the temperature increase would be larger in north than that in south, higher in the late-21st C than in the early. However, compared with mean temperature, the increase in extreme temperature is likely to be larger, particularly for minimum temperature. For example, the minimum temperature would increase exceeding 6 °C in the parts of northwestern China in the late-21st C.

3.2.2 Changes in annual cycles

The annual temperature cycles for the three future periods are shown in Figs. 7 and 8 for the five regions. The results show that the distribution shape (a single peak curve) of mean temperature in annual cycle in future is consistent with that in the baseline period (Fig. 7). It is noted that the spread among ensemble members is narrower in the first half of the year (especially from March to June) than the last 6 months for the next three periods. Figure 8 shows the mean temperature changes in the annual cycle relative to the baseline period. The monthly mean temperature rises consistently in the twenty-first century, with approximately [0.7, 2.0] °C in the early century, [2.0, 3.7] °C in the middle century and [3.3, 4.7] °C in the late century, as compared to the simulated baseline over the whole of China. For NE in middle and late twenty-first century, the change range is larger than that for other regions, especially in January, July, August, September and December (Fig. 8b). Although some members demonstrate slight or even negative temperature changes in NE for the early-21 C in the cold months (i.e., nearly zero in December). These small or even negative changes seem to be not at all evident in the spatial distribution of the temperature changes for this period in previous results (Figs. 5, 6b), which show the mean temperature increases obviously. It is not surprising because there are obvious positive temperature changes in other two months in winter, especially in January, and these positive changes contribute to the overall warming in this season. Similarly, previous results show the increase in spring is small (Fig. 6). From the annual cycle, we can find that the lowest temperature increase is in May of the year, in other words, the performance in May pulls down the overall mean temperature increment in this season.

Future changes in extreme temperature in annual cycle are analyzed preliminarily (Figure S8). The peak value of monthly mean extreme temperature over China appears in July, with about 20 °C for the minimum temperature and 30 °C for the maximum. The mean extreme temperature in January is the least. The mean minimum temperature would be below − 10 °C and the maximum is likely to be about 0 °C in future. The changes in extreme temperature during summer are larger than those in other months, which is inconsistent with the mean temperature (i.e., more increase in cold months). Similar with changes in spatial distribution, the amplitude in the minimum temperature is also larger than that in the maximum in annual cycle.

Moreover, the ensemble shows bigger variation in the late century (see long red boxes in Fig. 8) as compared to other two periods, which means that there are larger disagreements among simulations for long term projections.

3.2.3 Comparison with GCMs

In order to investigate whether the projections from PRECIS are consistent with GCM, we compare the downscaling outcomes to their driving GCMs. There is a basic agreement between them in projected temperature field distribution and warming trend (Figure S9). Again, the PRECIS shows its strength in the regional details, which are ignored

(a) China
(b) NE
(c) N
(d) SE
(e) W
°C
0.0
1.0
2.0
3.0
4.0
5.0
6.0
7.0
2020s
2050s
2080s
ANN
DJF
MAM
JJA
SON
1.7 3.2 4.6 1.8 3.4 4.8 1.4 2.7 4 1.7 3.4 4.7 1.7 3.3 4.7
1.9 3.6 5.1 2.2 4.2 5.7 1.6 2.8 4 1.9 3.8 5.1 2 3.8 5.4
1.5 3 4.4 1.8 2.9 4.3 1.3 2.6 3.9 1.5 3.2 4.5 1.5 3 4.4
1.3 2.7 3.9 1.4 2.4 3.7 1.1 2.4 3.5 1.3 2.9 3.9 1.3 2.8 4.1
1.6 3 4.4 1.8 3.4 4.8 1.4 2.8 3.6 1.3 2.9 4.4 1.7 3.3 4.5

◂**Fig. 6** Future changes in regional mean temperature in different seasons over the entire China (**a**) and sub-regions (**b**–**e**) compared to the baseline period (1961–1990) at 10% probability level (lower boundary), 50% probability level (dot, displaying numbers) and 90% probability level (upper boundary) in early, middle and late twenty-first century

or omitted in GCM owing to its low resolution, especially in the regions of immense complexity. For example, in most of southeastern regions, GCMs only show the two or three temperature ranges in rough, while the PRECIS provides much more information with the changes of terrain. On the other hand, during the baseline period, the PRECIS also shows more positive biases in most of China than GCMs (Fig. 2). It can be inferred that these biases in simulating present-day climate have not decreased with time and could be systematically propagated into future climate projection.

The comparisons of projected mean temperature changes in spatial distribution between the PRECIS and GCM ensemble are also carried out for three future periods (Figure S10). In general, the range of mean temperature changes in GCMs is larger than RCMs, particularly in the northeastern and northwestern regions. It seems that changes in temperature are less susceptible to a warming climate or less sensitiveness in climate change simulations that use RCMs than in simulations that use GCMs. Other researchers have made similar findings (Gao et al. 2011a, 2012b). The high-resolution RCM models may provide more land cover types, such as snow cover in the high latitudes or cold seasons. Under the background of climate warming, these land cover types would melt and absorb some heat, thus resulting in colder temperature than their driving GCMs.

3.2.4 Impacts of climate biases on projections

How the present-day known climates impact on its future unknown projection is sophisticated. Generally, there are two types of statistical biases in climate simulation. One is the deviation among models (i.e., bias between RCM and its driving GCM); the other is the actual biases (i.e., bias between simulation and observation). Two types of biases show very different effects on both baseline period and future trend projections. For the biases between RCM and its driving GCM, the spatial distributions in present-day simulation are obviously similar to corresponding future projections (Figure S11a–d), demonstrating that the bias from baseline period is almost totally transferred into future. However, their relationship maybe not exactly linear from the annual cycles (Figure S11e–i), though the overall trend is roughly identical. For example, over the northeast, the bias is obviously smaller from January to May in the middle century relative to other periods. For the actual biases based observation, the future changes are out line with the bias in the present-day simulation (Figure S12). In the spatial distribution, we cannot clearly identify the relationship between the cold or warm bias in baseline period and congruously warming trend in future. For example, over the northeast, the baseline bias is large in winter with the peak in February, whereas the changes are relatively small in the same month during three next periods. From May to October, the bias trend in baseline period is consistent with that in future periods, but the trend is opposite in other months. Over the west, the bias in the baseline is obviously smaller in warm months than in other months, but the projected change range in future seems to be not distinct and shows an overall stability.

4 Conclusions

In this study, a 25-km horizontal resolution regional climate model (PRECIS) is run over China from 1950 to 2099. Five GCMs are introduced as lateral boundary conditions to drive the PRECIS for further downscaling.

Overall, PRECIS can reasonably reproduce the observed temperature for most areas of China though simulations exhibit significant cold biases in the west, especially in the western edge of the Tibetan Plateau. PRECIS can well simulate mean temperature annual cycles over all regions, but the mean temperature over the whole country of China is underestimated throughout the year, especially in May and November. Compared to the PRECIS ensemble, the driving GCMs show relatively small biases in the west. Because RCMs could inherit some errors from GCMs in addition to their own errors, and these errors could be further magnified unintentionally when downscaling in western plateau regions. However, RCMs has a higher pattern correlation than GCMs owing to the enhanced representation of the land surface boundary.

Future temperature changes simulated by PRECIS for three successive 30-year periods in the twenty-first century are presented in this paper. The results indicate the following aspects:

1. In general, the ensemble regional simulations show an increase in mean temperature over all three time periods. On average for the whole of China, the temperature is likely to continue to increase throughout the twenty-first century (i.e., by [1.3, 1.9] °C in the early century, [2.5, 3.7] °C in the middle century, and [3.7, 5.2] °C) in the late century.
2. In the spatial distribution, there is an increasing pattern along with the latitude. The slightly change in temperature is found in spring and the warming trend in summer and winter (especially in winter) is more than the other seasons. On a monthly time-scale, monthly mean tem-

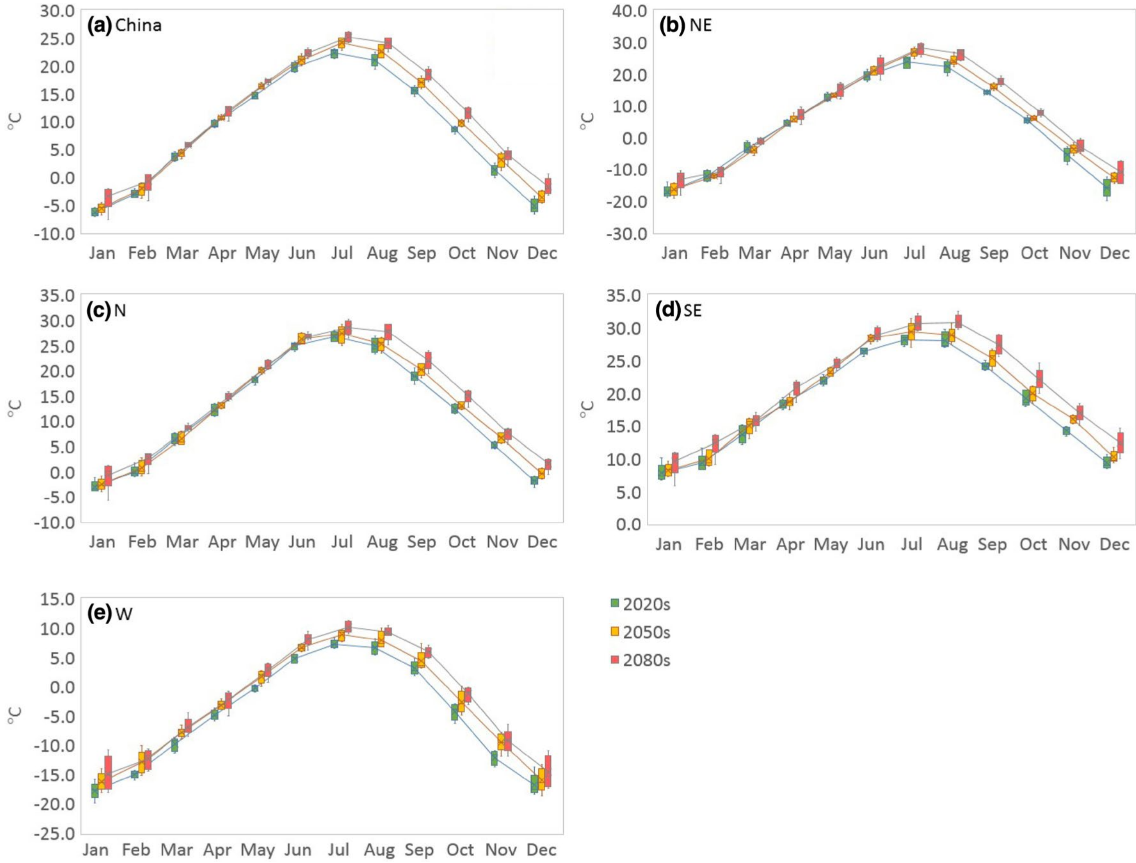

Fig. 7 Annual cycle of regional mean temperature over the whole China (**a**) and sub-regions (**b**–**e**) in early (blue), middle (yellow) and late (red) twenty-first century

perature will continue to rise over the next three periods, which is particularly obvious in the latter half of the year. Compared with other regions, the change range is larger in the north of China as well, especially in July, August and September. In addition, the change in mean temperature for some months (i.e., January, February and May) can dominate the corresponding seasonal changes. Moreover, this result also shows that there are larger disagreements among simulations for long term projections. Relative to mean temperature, the increase in extreme temperature is likely to be larger, particularly for minimum temperature. These changes are agreement with most studies (Wu et al. 2015; Xu et al. 2006; Zhou et al. 2014), which add confidence to our projection to some degree.

3. The projections in the distribution and tendency of climate change by PRECIS are consistent with the outcome form their driving GCMs. It also proved that the PRECIS shows better performance in incorporating more detailed information at finer spatial resolutions while representing good agreement with the spatio-temporal patterns of temperature changes projected by the driving GCMs. On the analysis on two biases in climate simulation, the biases derived from GCMs in present are systematically propagated into future climate projection. Though the overall trends are roughly identical, their relationship maybe not exactly linear. On the other hand, there is no apparent relationship between projected changes and model biases (i.e., larger bias does not necessarily lead to bigger changes in temperature).

It is important to assess the potential impacts and accurate prediction of future climate change, for developing targeted public policies and measures for adaptation and mitigation in the context of global warming. In this study, we highlight the strength of the high-resolution model in producing realistic small-scale features and the importance of an ensemble method in reducing uncertainties from models. We apply a high-resolution RCM ensemble method to explore the future changes in temperature over China and try to understand the uncertainties in climate model projections. The method could be applied to other regions of the globe, and these results could be directly used to analyze the impacts caused by climate warming on agriculture, energy and other related

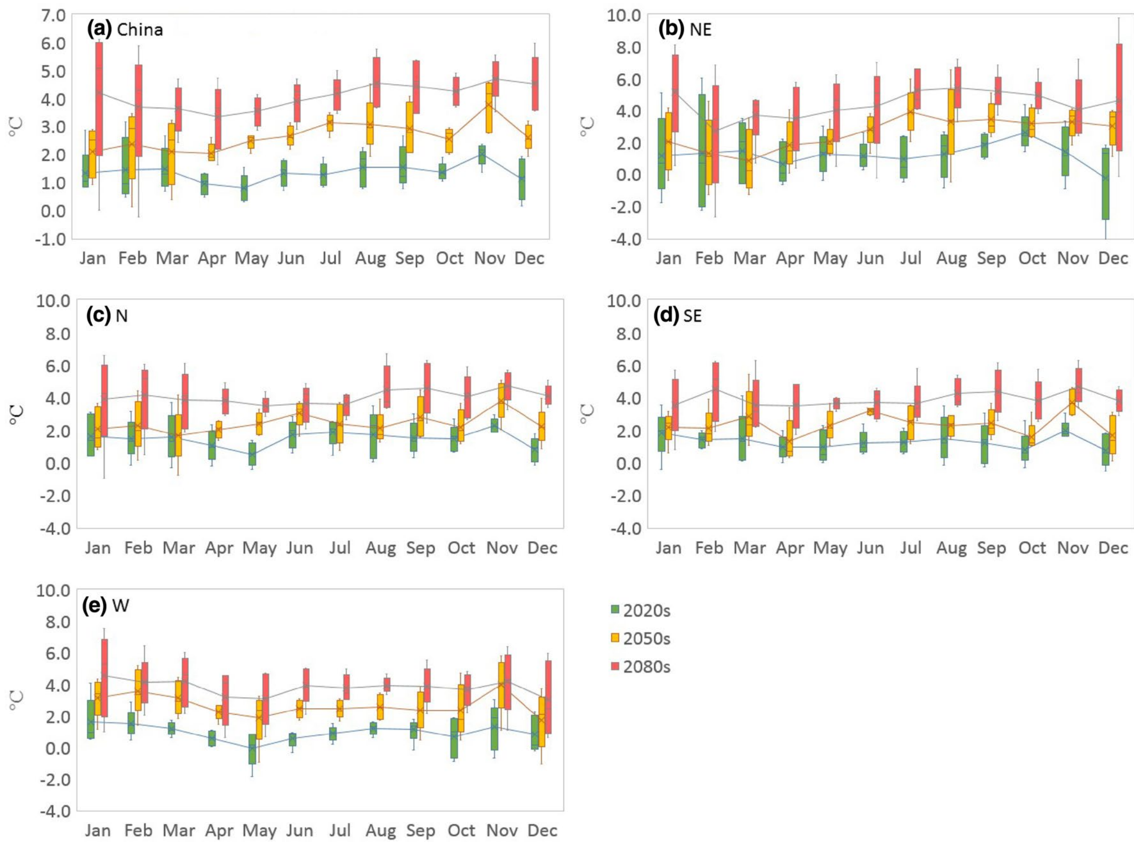

Fig. 8 Annual cycle of regional mean temperature changes over the whole China (**a**) and sub-regions (**b**–**e**) compared to the baseline period (1961–1990) in early (blue), middle (yellow) and late (red) twenty-first century

sectors in China. To a certain extent, the PRECIS model's downscaling can significantly improve the simulated ability of global climate models and yield more reliable future climate change prediction at regional and local scales, though the future projection should be interpreted with caution in complex topographical regions.

Acknowledgements This research was supported by the National Key Research and Development Plan (2016YFA0601502 and 2016YFC0502800), Fundamental Research Funds for the Central Universities (2017MS049), Environmental Protection Public Welfare Scientific Research Project (201509010).

References

Adger WN, Arnell NW, Tompkins EL (2005) Successful adaptation to climate change across scales. Glob Environ Chang 15:77–86

Boé J, Terray L, Habets F, Martin E (2007) Statistical and dynamical downscaling of the Seine basin climate for hydro-meteorological studies. Int J Climatol 27:1643–1655

Buontempo C, Mathison C, Jones R, Williams K, Wang C, Mcsweeney C (2014) An ensemble climate projection for Africa. Clim Dyn 44:1–22

Chen X, Hu B, Yu R (2005) Spatial and temporal variation of phenological growing season and climate change impacts in temperate eastern China. Glob Change Biol 11:1118–1130

Collins M, Booth BB, Harris GR, Murphy JM, Sexton DM, Webb MJ (2006) Towards quantifying uncertainty in transient climate change. Clim Dyn 27:127–147

Di W, Yong Z, Pei YS (2010) Numerical simulation and evaluation of regional climate change in southwest China by a regional climate model. Procedia Environ Sci 2:1540–1554

Gao Y, Vano JA, Zhu C, Lettenmaier DP (2011a) Evaluating climate change over the Colorado River basin using regional climate models. J Geophys Res 116:D13104

Gao Y, Xue Y, Peng W, Kang H, Waliser D (2011b) Assessment of dynamic downscaling of china regional summer climate using regional climate model. Adv Atmos Sci 28(5):1077–1098

Gao X, Shi Y, Zhang D, Giorgi F (2012a) Climate change in China in the 21st century as simulated by a high resolution regional climate model. Chin Sci Bull 57:1188–1195

Gao Y, Leung LR, Salathé EP Jr, Dominguez F, Nijssen B, Lettenmaier DP (2012b) Moisture flux convergence in regional and global climate models: implications for droughts in the southwestern United States under climate change. Geophys Res Lett 39:L09711

Gao Y, Xu J, Chen D (2015) Evaluation of WRF mesoscale climate simulations over the tibetan plateau during 1979–2011. J Clim 28(1):2823–2841. https://doi.org/10.1175/JCLI-D-14-00300.1

Guo J, Huang G, Wang X, Lin Q (2017) Investigating future precipitation changes over China through a high-resolution regional climate model ensemble. Earth's Future. https://doi.org/10.1002/2016EF000433

Guo J, Huang G, Wang X, Li Y, Yang L (2018) Future changes in precipitation extremes over china projected by a regional climate model ensemble. Atmos Environ 188:142–156

Hamada A, Arakawa O, Yatagai A (2011) An automated quality control method for daily rain-gauge data. Glob Environ Res V15N2:183–192

Huang WR, Chan JC, Au-Yeung AY (2013) Regional climate simulations of summer diurnal rainfall variations over East Asia and Southeast China. Clim Dyn 40(7–8):1625–1642

Jiang Z, Li W, Xu J, Li L (2015) Extreme precipitation indices over china in cmip5 models. Part I: model evaluation. J Clim 28(21):150902151739009

Liang X, Kunkel KE, Meehl GA, Jones RG, Wang JXL (2008) Regional climate models downscaling analysis of general circulation models present climate biases propagation into future change projections. Geophys Res Lett 35(8):193–202

Liu S, Gao W, Liang XZ (2013) A regional climate model downscaling projection of China future climate change. Clim Dyn 41:1871–1884

McSweeney CF, Jones RG (2010) Selecting members of the 'QUMP' perturbed-physics ensemble for use with PRECIS. MetOffice Hadley Centre, Devon, p 9

McSweeney CF, Jones RG, Booth BB (2012) Selecting ensemble members to provide regional climate change information. J Clim 25(20):7100–7121

Murphy JM Coauthors (2009) UK climate projections science report: climate change projections. Met Office, Exeter, p 193

Ouyang W, Shi Y, Hao F, Jiao W (2015) A comparison of general circulation models and their application to temperature change assessments in a high-latitude agricultural area in northeastern China. Clim Dyn 47:1–16

Redmond G, Hodges KI, Mcsweeney C, Jones R, Hein D (2015) Projected changes in tropical cyclones over Vietnam and the south China sea using a 25 km regional climate model perturbed physics ensemble. Clim Dyn 45:1–18

Shi YF, Shen YP, Li DL, Zhang GW, Ding YJ, Hu RJ, Kang ES (2003) Discussion on the present climate change from warm-dry to warm-wet in northwest China. Quat Sci 23:152–164

Shi Y, Shen Y, Kang E, Li D, Ding Y, Zhang G, Hu R (2007) Recent and future climate change in northwest China. Clim Change 80:379–393

Taylor KE (2001) Summarizing multiple aspects of model performance in a single diagram. J Geophys Res 106:7183–7192

Wang X, Huang G, Lin Q, Liu J (2014a) High-resolution probabilistic projections of temperature changes over Ontario, Canada. J Clim 27:5259–5284

Wang Z, Duan A, Wu G (2014b) Time-lagged impact of spring sensible heat over the Tibetan plateau on the summer rainfall anomaly in east China: case studies using the WRF model. Clim Dyn 42:2885–2898

Wang X, Huang G, Liu J (2015) Twenty-first century probabilistic projections of precipitation over Ontario, Canada through a regional climate model ensemble. Clim Dyn 46:1–23

Wu J, Gao X-J, Xu Y-L, Pan J (2015) Regional climate change and uncertainty analysis based on four regional climate model simulations over China. Atmos Oceanic Sci Lett 8(3):147–152

Xu YL, Pan J, Feng Q (2006) Projection on future climate change in China-constructing high resolution SRES climate scenarios using PRECIS. Science, Beijing

Yu E, Sun J, Chen H, Xiang W (2014) Evaluation of a high-resolution historical simulation over China: climatology and extremes. Clim Dyn 45:1–19

Zhou B, Wen QH, Xu Y, Song L (2014) Projected changes in temperature and precipitation extremes in China by the CMIP5 multimodel ensembles. J Clim 27:6591–6611

Affiliations

Junhong Guo[1] · Guohe Huang[2,3] · Xiuquan Wang[4] · Yongping Li[5]

[1] MOE Key Laboratory of Resource and Environmental System Optimization, College of Environmental Science and Engineering, North China Electric Power University, Beijing 102206, China

[2] Institute for Energy, Environment and Sustainable Communities, University of Regina, Regina, SK S4S 0A2, Canada

[3] Center for Energy, Environment and Ecology Research, UR-BNU, Beijing Normal University, Beijing 100875, China

[4] School of Climate Change and Adaptation, University of Prince Edward Island, Charlottetown, PE C1A 4P3, Canada

[5] School of Environment, Beijing Normal University, Beijing 100875, China